KTA1

Slides to lectures 20/25.11.2013

Wiederholung & Zusammenfassung

Wirkungsquerschnitt: „wirksame" Querschnittsfläche eines Targetpartikel (Einheit: 1 barn = 1E-24 cm ^{2}

Elastische Streuung an Elektronen: **Thomson Querschnitt**: $\sigma_{Th} = (8\pi/3)\, r_e^2 \approx$ 0.7 barn; klassischer Elektronen-radius: r_e = 2.8 fm

Photoelektrische Effekt: $T = E_\gamma - B_E$;

- T =: kinetische Energie des Elektrons
- E_γ : Energie des Photons
- B_E : Bindungsenergie des Elektrons

Photo-Effekt dominiert bei $E_\gamma < \approx 100$ keV

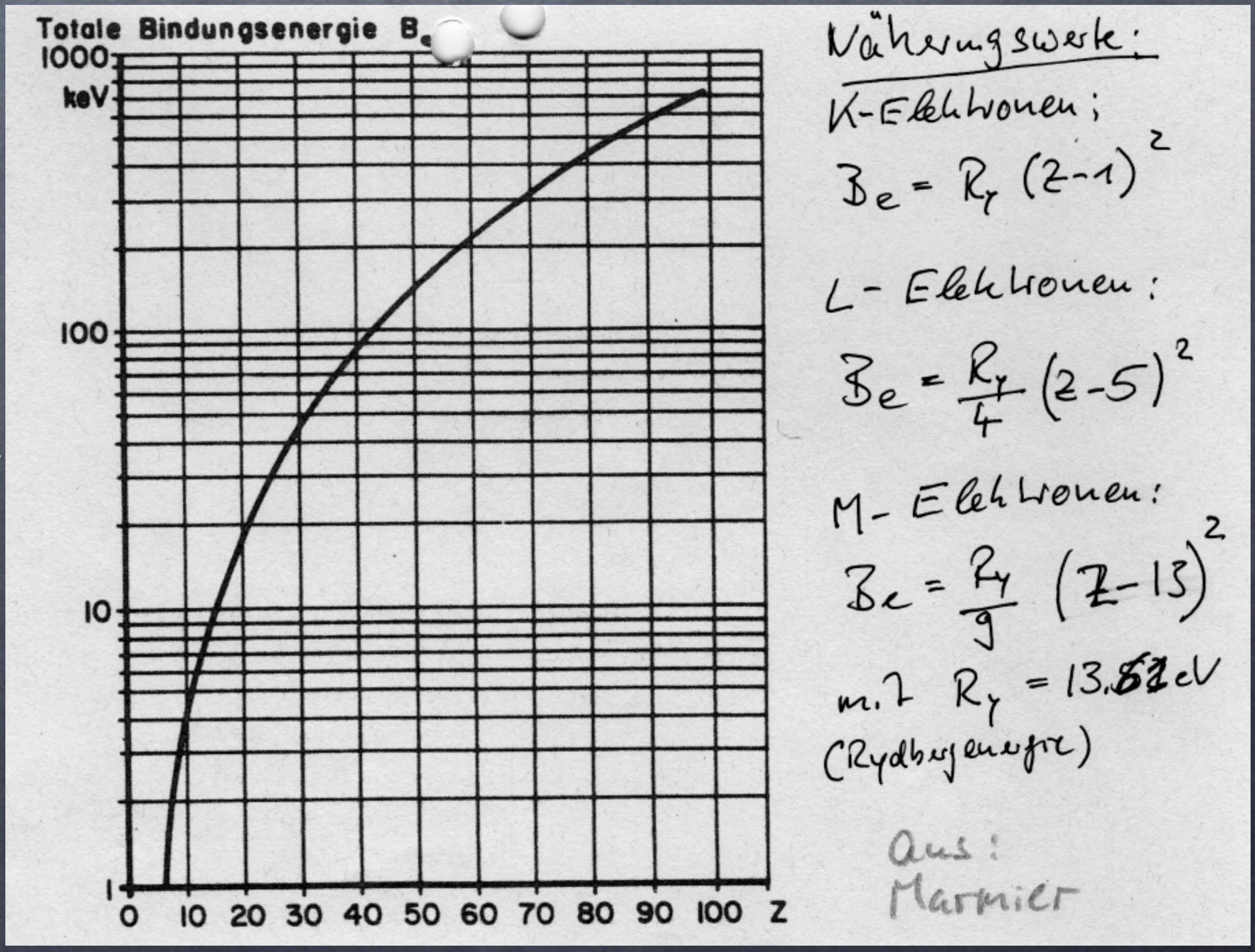

Streuung an Elektronen der Atomhülle:

Compton Streuung: Streuung an freien Elektronen

WQ mittels QED:
Klein-Nishina-Gleichung:

$$\frac{d\sigma}{d\Omega} = \frac{r_e^2}{2}\frac{1}{\left[1+\gamma(1-\cos\theta)\right]^2}\left(1+\cos^2\theta+\frac{\gamma^2(1-\cos\theta)^2}{1+\gamma(1-\cos\theta)}\right)$$

mit $\gamma = E_\gamma / m_e c^2$

Maximale Energie des gestreuten Elektrons:

$$T_{max} = E_\gamma \frac{2\gamma}{1+2\gamma}$$

Differentielle WQ:

$$\frac{d\sigma}{dT} = \frac{\pi r_e^2}{m_e\gamma^2}\left[2+\frac{s^2}{\gamma^2(1-s)^2}+\frac{s}{1-s}\left(s-\frac{2}{\gamma}\right)\right]$$

mit $s = T/E_\gamma$

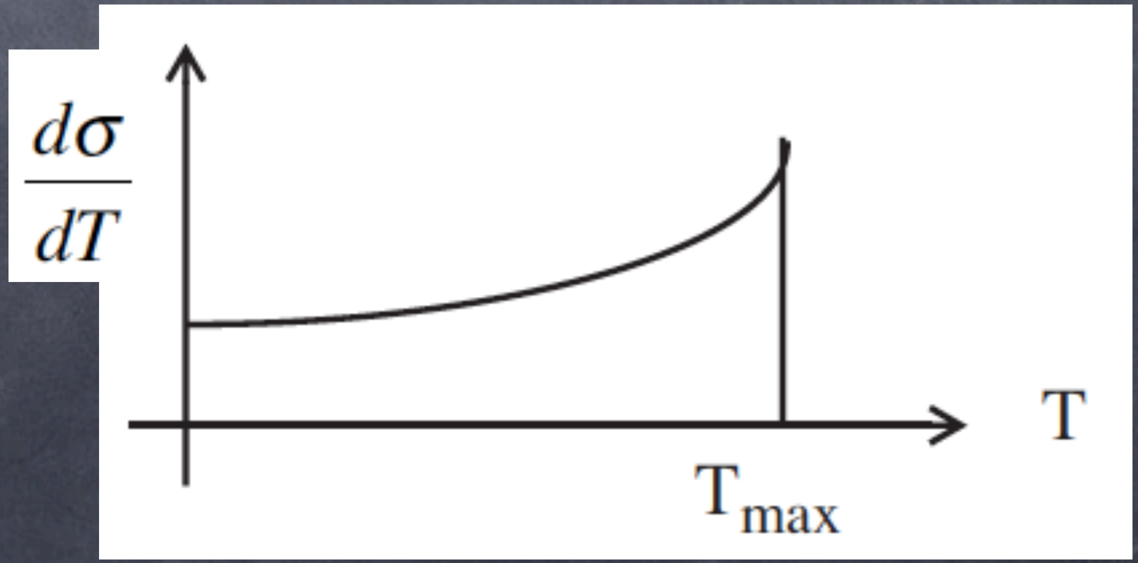

Paarerzeugung: $E_\gamma > 2m_e \approx 1.02$ MeV

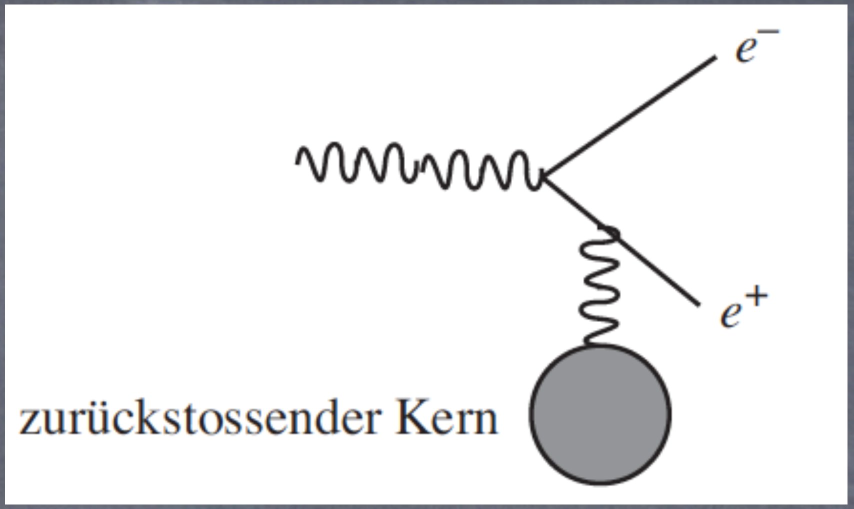

Um Impuls- und Energieerhaltung zu gewährleisten:
Nur möglich in Anwesenheit eines Kerns

WQ:

$$\sigma_{Paar} \approx \left(4\alpha r_e^2\right) Z^2 \left(\frac{7}{9} \ln \frac{183}{Z^{1/3}}\right)$$

Kernphoto-Effekt: Selten im Vergleich mit anderen Photoreaktionen. Photon wird von Kern absorbiert und falls $E_\gamma > B_{nucleon}$ bevorzugt Neutronen emittiert (vgl. Bild des Potentialtopfs Fermi-Modell)

WQ von Photonen als Funktion der Energie für C (Z=12) und Blei (Z=82)

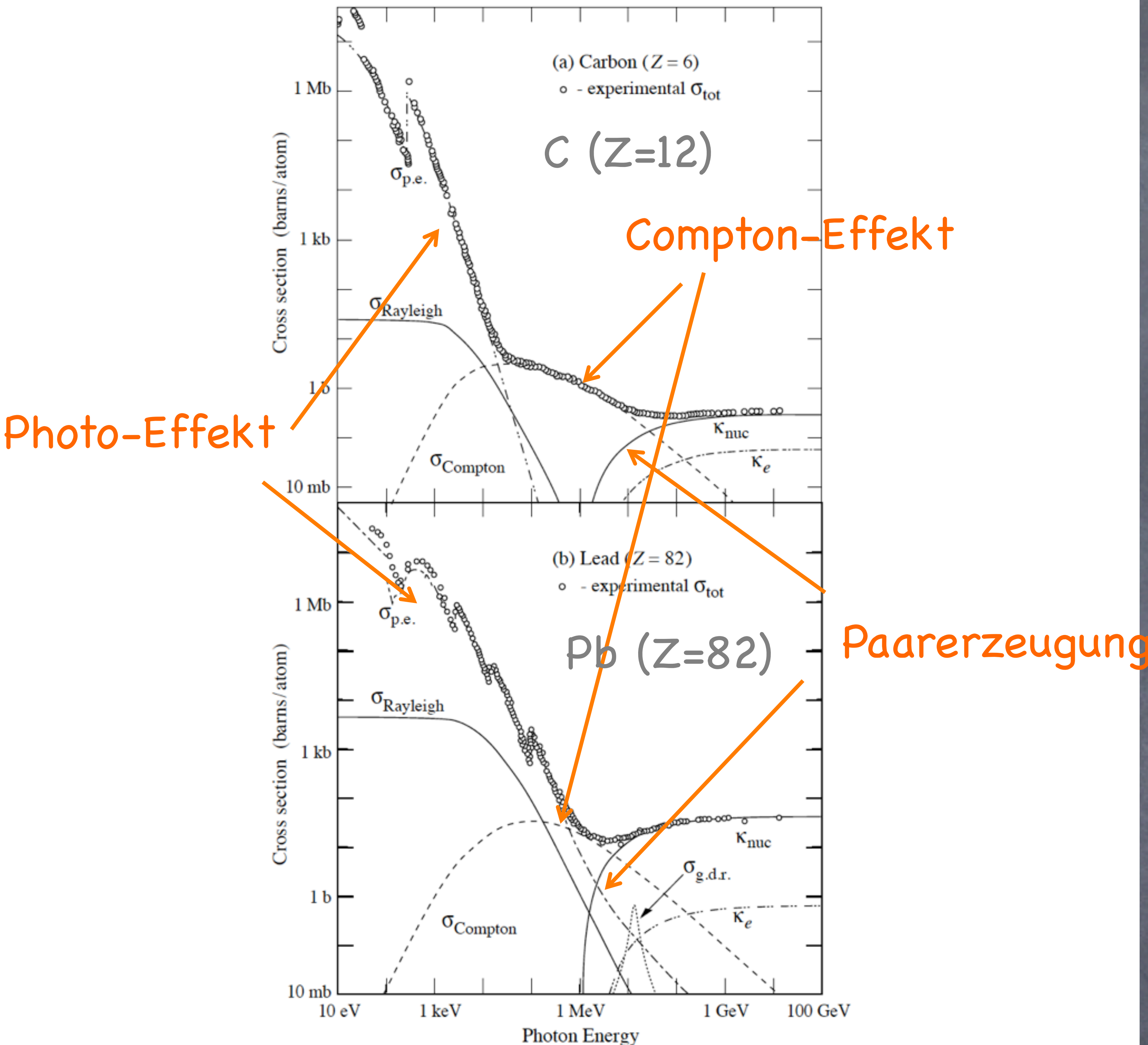

Figure 30.15: Photon total cross sections as a function of energy in carbon and lead, showing the contributions of different processes [48]:

$\sigma_{\text{p.e.}}$ = Atomic photoelectric effect (electron ejection, photon absorption)
σ_{Rayleigh} = Rayleigh (coherent) scattering–atom neither ionized nor excited
σ_{Compton} = Incoherent scattering (Compton scattering off an electron)
κ_{nuc} = Pair production, nuclear field
κ_e = Pair production, electron field
$\sigma_{\text{g.d.r.}}$ = Photonuclear interactions, most notably the Giant Dipole Resonance [49]. In these interactions, the target nucleus is broken up.

Original figures through the courtesy of John H. Hubbell (NIST).

J. Beringer *et al.*(PDG), PR **D86**, 010001 (2012) (http://pdg.lbl.gov)

Abschwächlänge bzw. mittlere freie Weglänge von Photonen

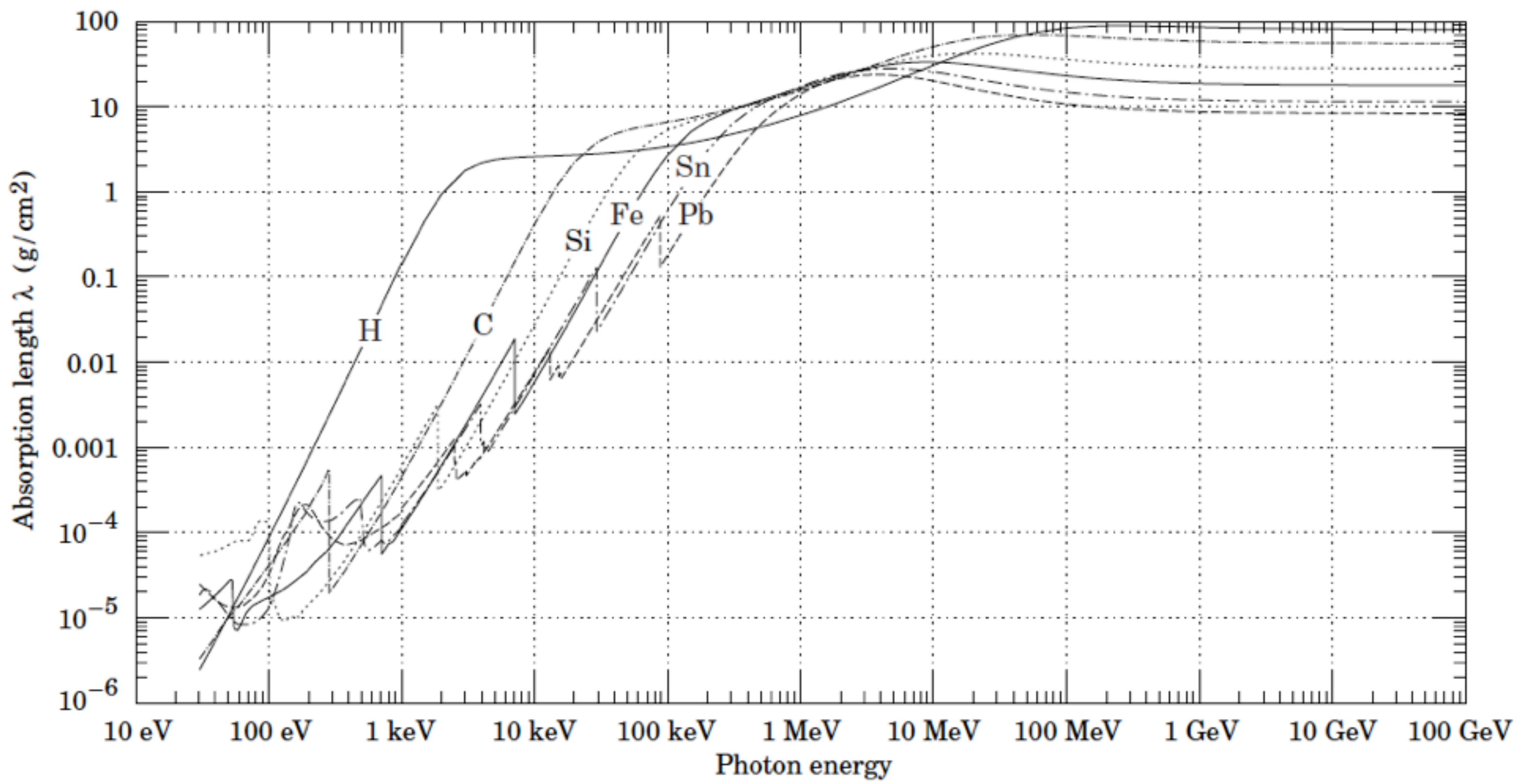

Figure 30.16: The photon mass attenuation length (or mean free path) $\lambda = 1/(\mu/\rho)$ for various elemental absorbers as a function of photon energy. The mass attenuation coefficient is μ/ρ, where ρ is the density. The intensity I remaining after traversal of thickness t (in mass/unit area) is given by $I = I_0 \exp(-t/\lambda)$. The accuracy is a few percent. For a chemical compound or mixture, $1/\lambda_{\text{eff}} \approx \sum_{\text{elements}} w_Z/\lambda_Z$, where w_Z is the proportion by weight of the element with atomic number Z. The processes responsible for attenuation are given in Fig. 30.11. Since coherent processes are included, not all these processes result in energy deposition. The data for 30 eV $< E <$ 1 keV are obtained from `http://www-cxro.lbl.gov/optical_constants` (courtesy of Eric M. Gullikson, LBNL). The data for 1 keV $< E <$ 100 GeV are from `http://physics.nist.gov/PhysRefData`, through the courtesy of John H. Hubbell (NIST).

J. Beringer *et al.*(PDG), PR **D86**, 010001 (2012) (http://pdg.lbl.gov)

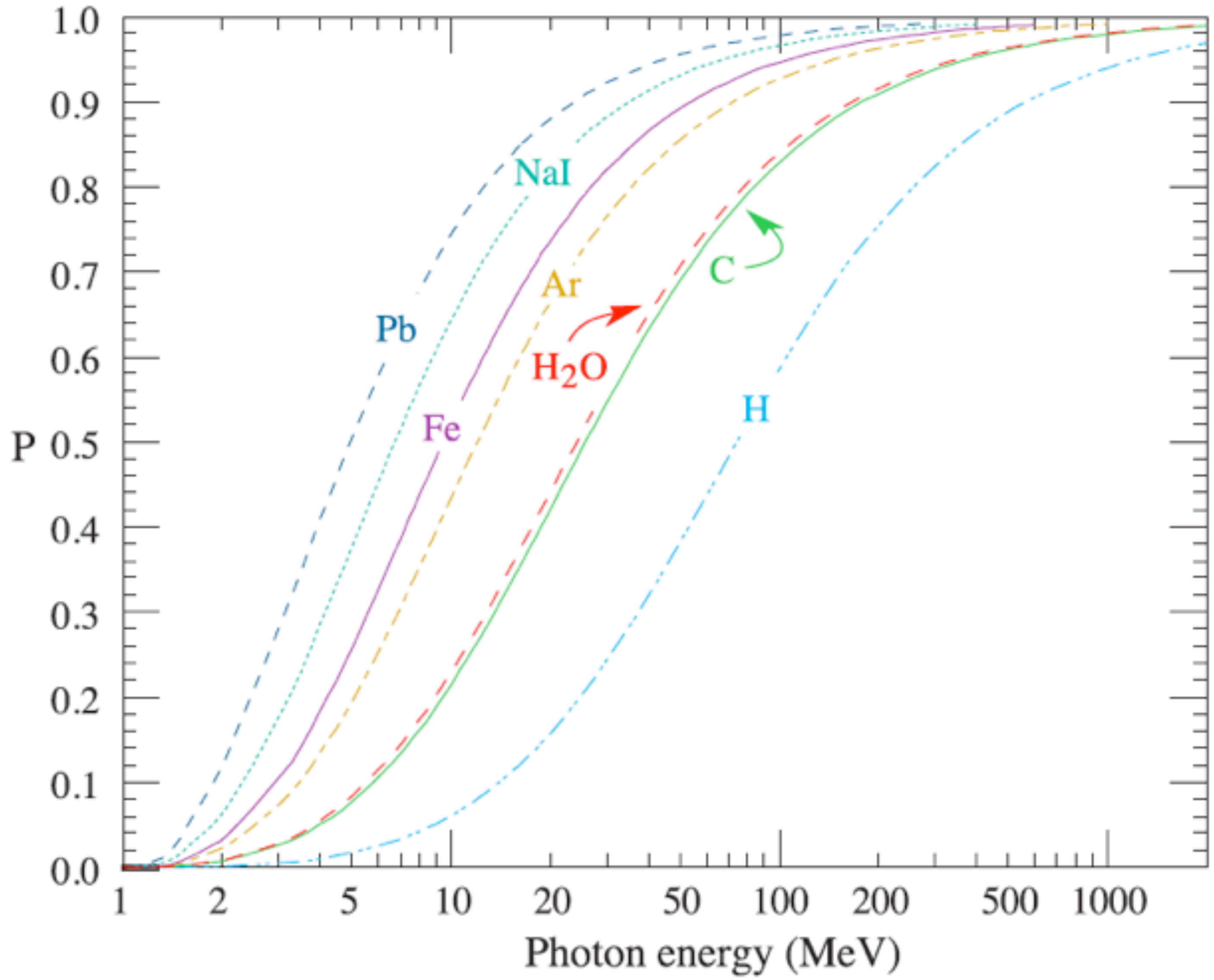

Figure 30.17: Probability P that a photon interaction will result in conversion to an e^+e^- pair. Except for a few-percent contribution from photonuclear absorption around 10 or 20 MeV, essentially all other interactions in this energy range result in Compton scattering off an atomic electron. For a photon attenuation length λ (Fig. 30.16), the probability that a given photon will produce an electron pair (without first Compton scattering) in thickness t of absorber is $P[1 - \exp(-t/\lambda)]$.

J. Beringer *et al.*(PDG), PR **D86**, 010001 (2012) (http://pdg.lbl.gov)

http://pdg.lbl.gov/2013/reviews/rpp2012-rev-atomic-nuclear-prop.pdf

6. ATOMIC AND NUCLEAR PROPERTIES OF MATERIALS

Table 6.1 Abridged from `pdg.lbl.gov/AtomicNuclearProperties` by D. E. Groom (2007). See web pages for more detail about entries in this table including chemical formulae, and for several hundred other entries. Quantities in parentheses are for NTP (20° C and 1 atm), and square brackets indicate quantities evaluated at STP. Boiling points are at 1 atm. Refractive indices n are evaluated at the sodium D line blend (589.2 nm); values $\gg$1 in brackets are for $(n-1)\times 10^6$ (gases).

Material	Z	A	$\langle Z/A\rangle$	Nucl.coll. length λ_T {g cm^{-2}}	Nucl.inter. length λ_I {g cm^{-2}}	Rad.len. X_0 {g cm^{-2}}	$dE/dx\|_{min}$ { MeV g^{-1}cm^2}	Density {g cm^{-3}} ({gℓ^{-1}})	Melting point (K)	Boiling point (K)	Refract. index (@ Na D)
H_2	1	1.00794(7)	0.99212	42.8	52.0	63.04	(4.103)	0.071(0.084)	13.81	20.28	1.11[132.]
D_2	1	2.01410177803(8)	0.49650	51.3	71.8	125.97	(2.053)	0.169(0.168)	18.7	23.65	1.11[138.]
He	2	4.002602(2)	0.49967	51.8	71.0	94.32	(1.937)	0.125(0.166)		4.220	1.02[35.0]
Li	3	6.941(2)	0.43221	52.2	71.3	82.78	1.639	0.534	453.6	1615.	
Be	4	9.012182(3)	0.44384	55.3	77.8	65.19	1.595	1.848	1560.	2744.	
C diamond	6	12.0107(8)	0.49955	59.2	85.8	42.70	1.725	3.520			2.42
C graphite	6	12.0107(8)	0.49955	59.2	85.8	42.70	1.742	2.210			
Fe	26	55.845(2)	0.46557	81.7	132.1	13.84	1.451	7.874	1811.	3134.	
Cu	29	63.546(3)	0.45636	84.2	137.3	12.86	1.403	8.960	1358.	2835.	
Ge	32	72.64(1)	0.44053	86.9	143.0	12.25	1.370	5.323	1211.	3106.	
Sn	50	118.710(7)	0.42119	98.2	166.7	8.82	1.263	7.310	505.1	2875.	
Xe	54	131.293(6)	0.41129	100.8	172.1	8.48	(1.255)	2.953(5.483)	161.4	165.1	1.39[701.]
W	74	183.84(1)	0.40252	110.4	191.9	6.76	1.145	19.300	3695.	5828.	
Pt	78	195.084(9)	0.39983	112.2	195.7	6.54	1.128	21.450	2042.	4098.	
Au	79	196.966569(4)	0.40108	112.5	196.3	6.46	1.134	19.320	1337.	3129.	
Pb	82	207.2(1)	0.39575	114.1	199.6	6.37	1.122	11.350	600.6	2022.	
U	92	[238.02891(3)]	0.38651	118.6	209.0	6.00	1.081	18.950	1408.	4404.	
Air (dry, 1 atm)			0.49919	61.3	90.1	36.62	(1.815)	(1.205)		78.80	
Shielding concrete			0.50274	65.1	97.5	26.57	1.711	2.300			
Borosilicate glass (Pyrex)			0.49707	64.6	96.5	28.17	1.696	2.230			
Lead glass			0.42101	95.9	158.0	7.87	1.255	6.220			
Standard rock			0.50000	66.8	101.3	26.54	1.688	2.650			
Water (H_2O)			0.55509	58.5	83.3	36.08	1.992	1.000(0.756)	273.1	373.1	1.33

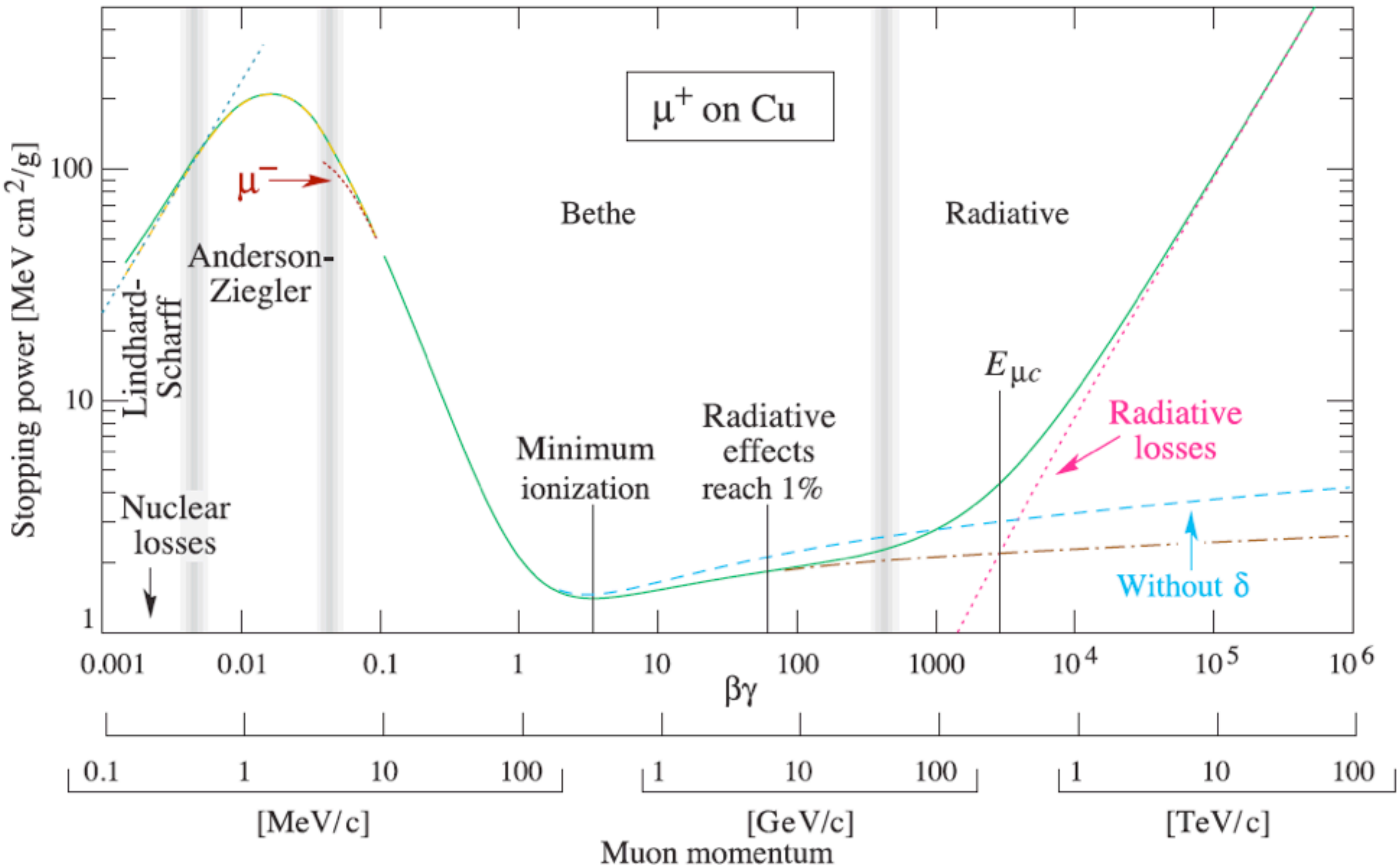

Fig. 30.1: Stopping power ($= \langle -dE/dx \rangle$) for positive muons in copper as a function of $\beta\gamma = p/Mc$ over nine orders of magnitude in momentum (12 orders of magnitude in kinetic energy). Solid curves indicate the total stopping power. Data below the break at $\beta\gamma \approx 0.1$ are taken from ICRU 49 [4], and data at higher energies are from Ref. 5. Vertical bands indicate boundaries between different approximations discussed in the text. The short dotted lines labeled "μ^-" illustrate the "Barkas effect," the dependence of stopping power on projectile charge at very low energies [6].

J. Beringer *et al.*(PDG), PR **D86**, 010001 (2012) (http://pdg.lbl.gov)

$$-\left\langle \frac{dE}{dx} \right\rangle = K z^2 \frac{Z}{A} \frac{1}{\beta^2} \left[\frac{1}{2} \ln \frac{2 m_e c^2 \beta^2 \gamma^2 T_{\max}}{I^2} - \beta^2 - \frac{\delta(\beta\gamma)}{2} \right]$$

Bethe-Bloch

Für: $0.1 \lesssim \beta\gamma \lesssim 1000$

30.1. Notation

Table 30.1: Summary of variables used in this section. The kinematic variables β and γ have their usual meanings.

Symbol	Definition	Units or Value
α	Fine structure constant $(e^2/4\pi\epsilon_0\hbar c)$	1/137.035 999 11(46)
M	Incident particle mass	MeV/c^2
E	Incident part. energy γMc^2	MeV
T	Kinetic energy	MeV
m_ec^2	Electron mass $\times$ c^2	0.510 998 918(44) MeV
r_e	Classical electron radius $e^2/4\pi\epsilon_0 m_ec^2$	2.817 940 325(28) fm
N_A	Avogadro's number	6.022 1415(10) $\times 10^{23}$ mol^{-1}
ze	Charge of incident particle	
Z	Atomic number of absorber	
A	Atomic mass of absorber	g mol^{-1}
K/A	$4\pi N_A r_e^2 m_ec^2/A$	0.307 075 MeV g^{-1} cm^2 for A = 1 g mol^{-1}
I	Mean excitation energy	eV (*Nota bene!*)
$\delta(\beta\gamma)$	Density effect correction to ionization energy loss	
$\hbar\omega_p$	Plasma energy $(\sqrt{4\pi N_e r_e^3}\ m_ec^2/\alpha)$	$\sqrt{\rho\langle Z/A\rangle} \times 28.816$ eV (ρ in g cm^{-3})
N_e	Electron density	(units of r_e)$^{-3}$
w_j	Weight fraction of the jth element in a compound or mixture	
n_j	$\propto$ number of jth kind of atoms in a compound or mixture	
—	$4\alpha r_e^2 N_A/A$	(716.408 g cm^{-2})$^{-1}$ for $A = 1$ g mol^{-1}
X_0	Radiation length	g cm^{-2}
E_c	Critical energy for electrons	MeV
$E_{\mu c}$	Critical energy for muons	GeV
E_s	Scale energy $\sqrt{4\pi/\alpha}\ m_ec^2$	21.2052 MeV
R_M	Molière radius	g cm^{-2}

J. Beringer *et al.*(PDG), PR **D86**, 010001 (2012) (http://pdg.lbl.gov)

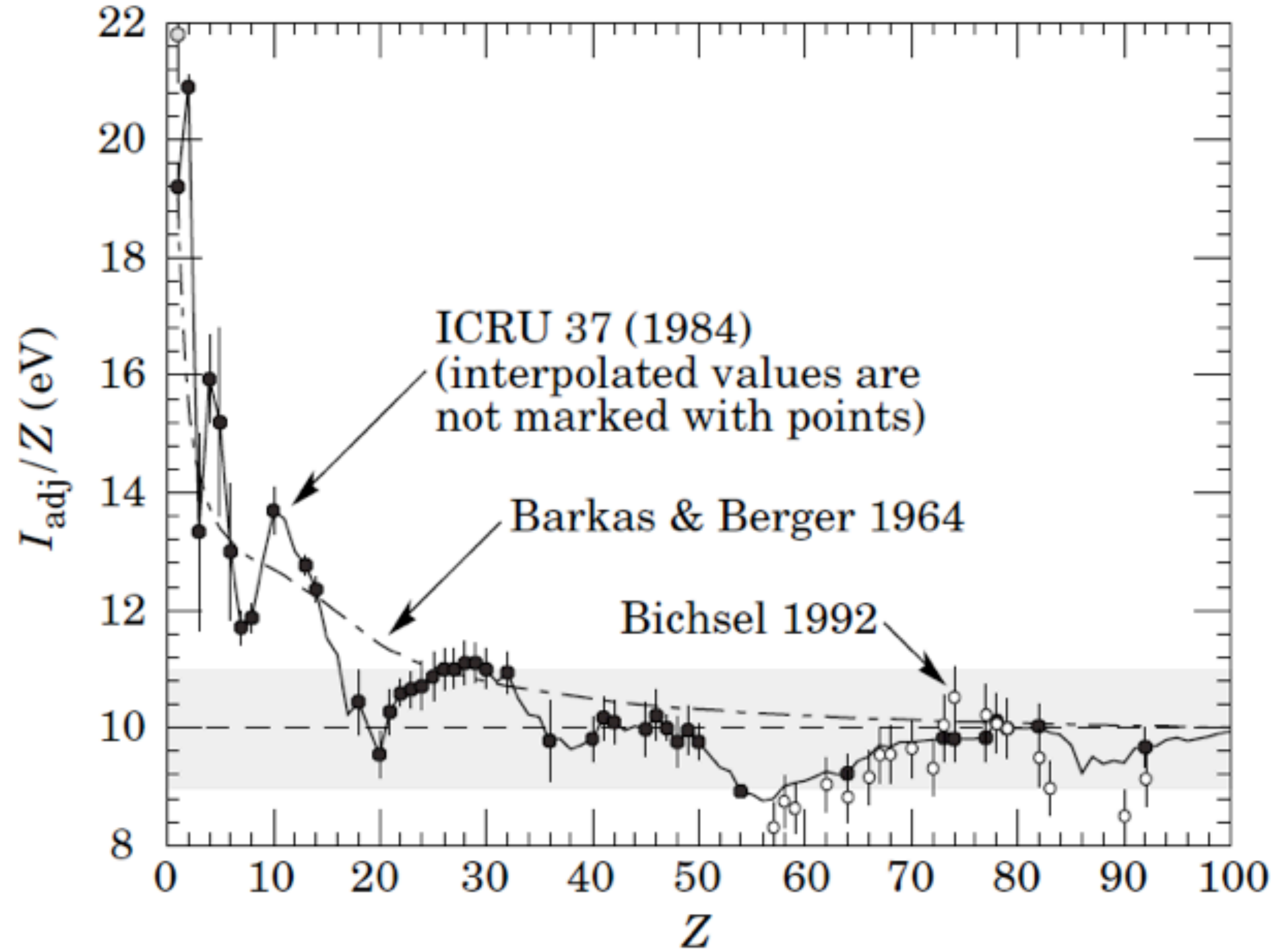

Figure 30.5: Mean excitation energies (divided by Z) as adopted by the ICRU [11]. Those based on experimental measurements are shown by symbols with error flags; the interpolated values are simply joined. The grey point is for liquid H_2; the black point at 19.2 eV is for H_2 gas. The open circles show more recent determinations by Bichsel [13]. The dotted curve is from the approximate formula of Barkas [14] used in early editions of this *Review*.

J. Beringer *et al.*(PDG), PR **D86**, 010001 (2012) (http://pdg.lbl.gov)

Bragg peak
Energiedeposition C-Ionen vs Photons

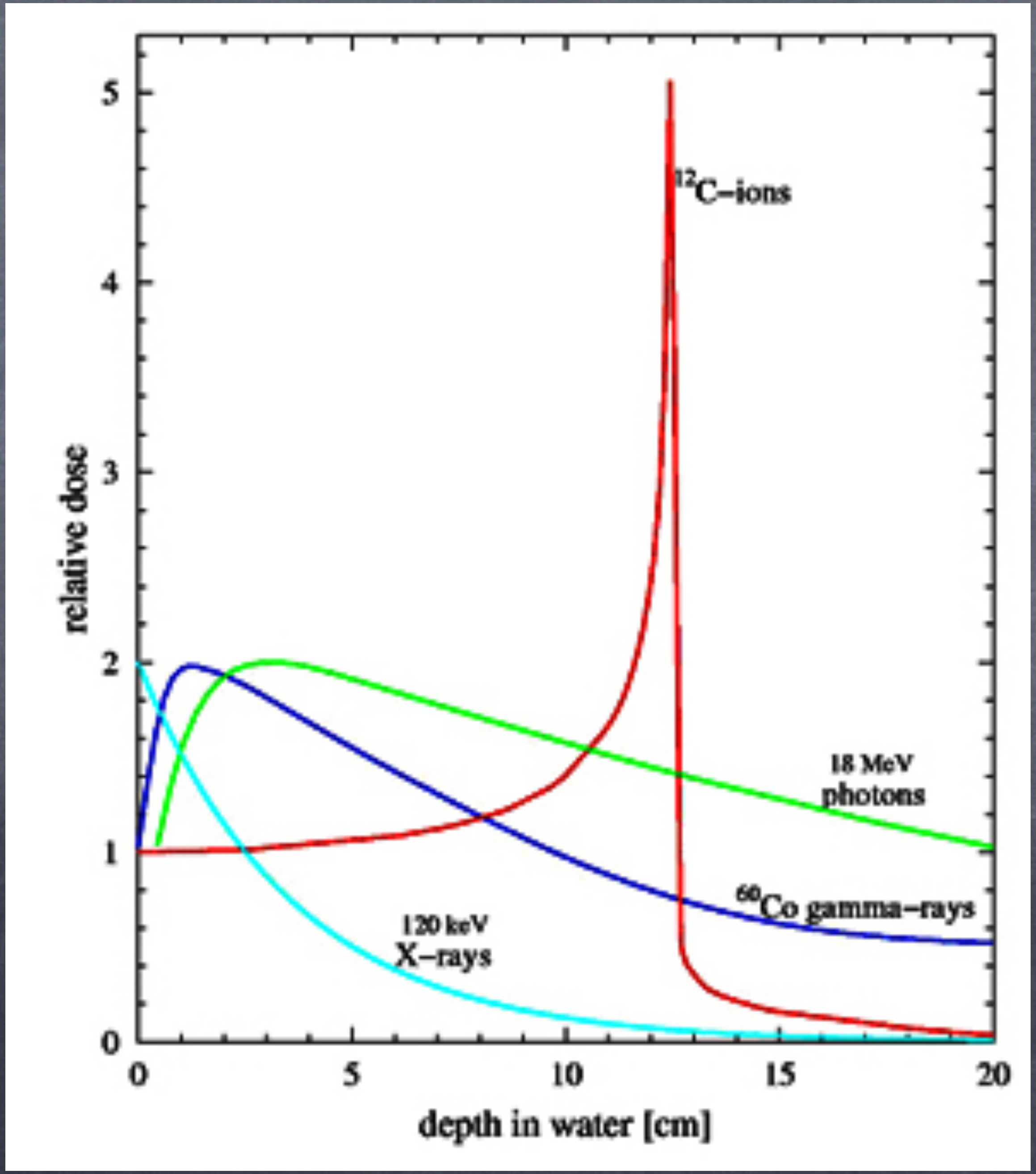

Bragg Kurve & Strahlentherapie

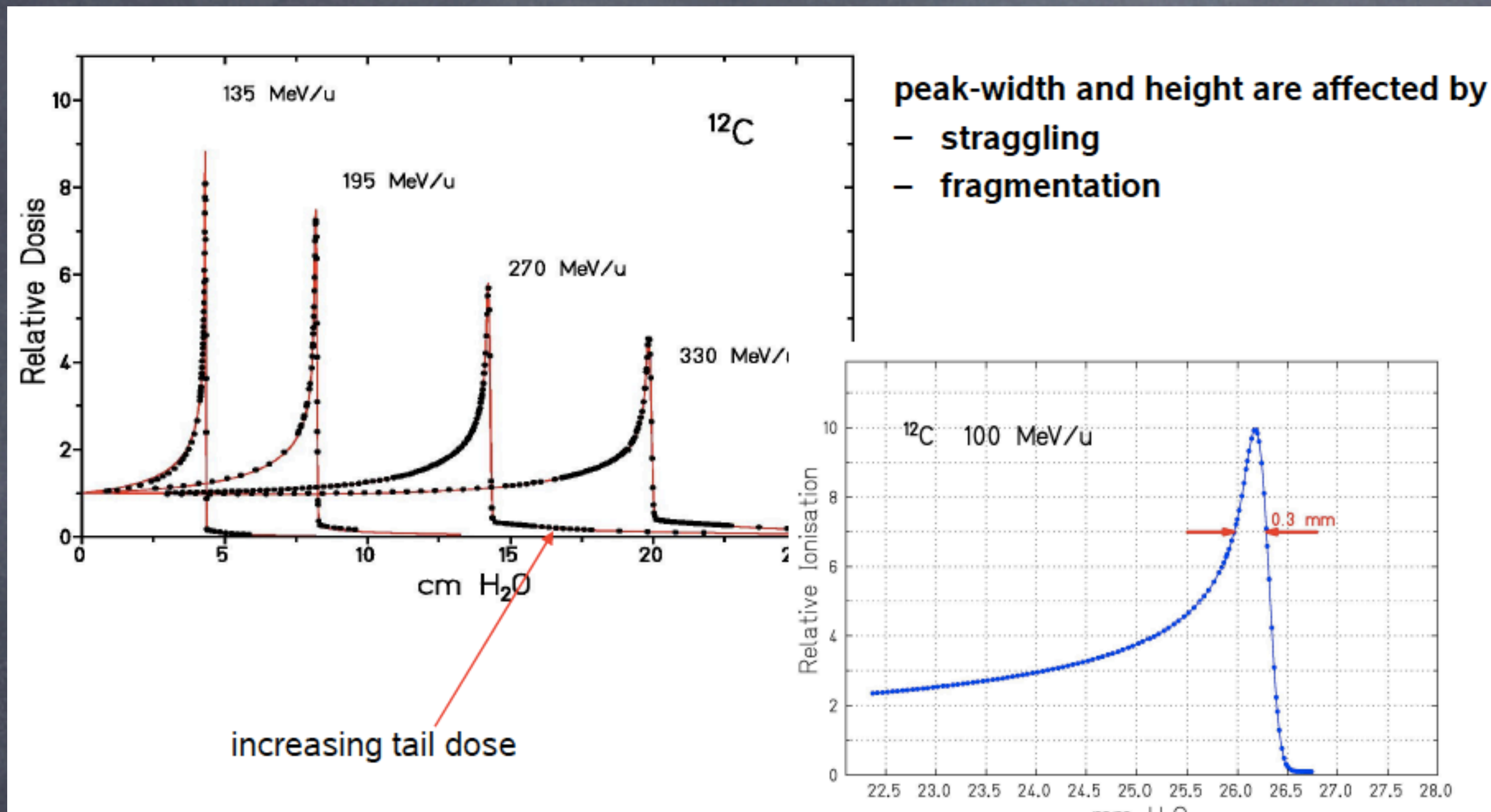

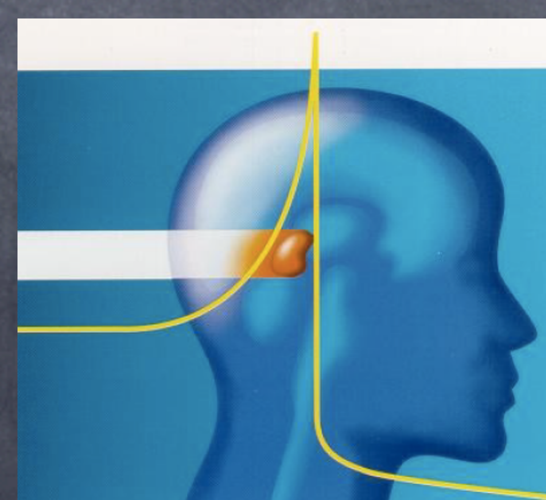

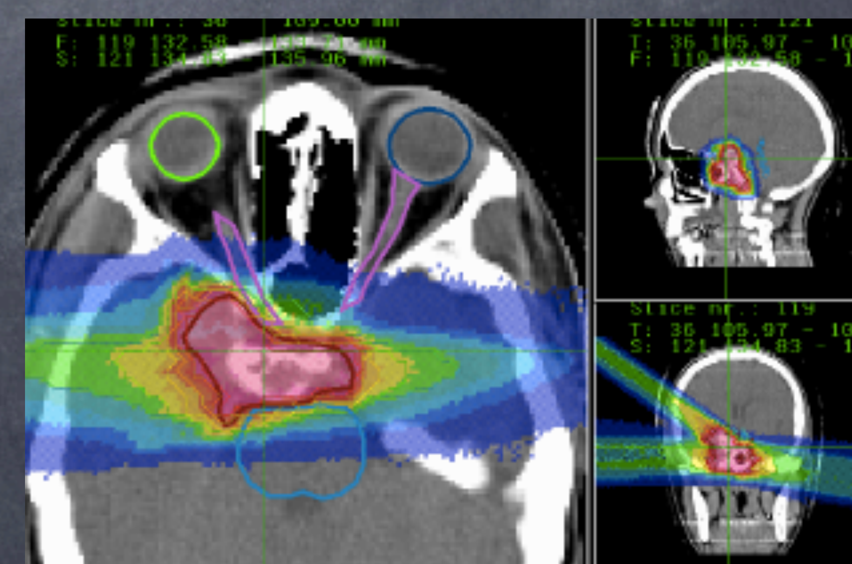

Table 30.1: Summary of variables used in this section. The kinematic variables β and γ have their usual meanings.

Symbol	Definition	Units or Value
α	Fine structure constant $(e^2/4\pi\epsilon_0\hbar c)$	$1/137.035\,999\,11(46)$
M	Incident particle mass	MeV/c^2
E	Incident part. energy $\gamma M c^2$	MeV
T	Kinetic energy	MeV
$m_e c^2$	Electron mass $\times\ c^2$	$0.510\,998\,918(44)$ MeV
r_e	Classical electron radius $e^2/4\pi\epsilon_0 m_e c^2$	$2.817\,940\,325(28)$ fm
N_A	Avogadro's number	$6.022\,1415(10) \times 10^{23}$ mol^{-1}
ze	Charge of incident particle	
Z	Atomic number of absorber	
A	Atomic mass of absorber	g mol^{-1}
K/A	$4\pi N_A r_e^2 m_e c^2/A$	$0.307\,075$ MeV g^{-1} cm^2 for A = 1 g mol^{-1}
I	Mean excitation energy	eV (*Nota bene!*)
$\delta(\beta\gamma)$	Density effect correction to ionization energy loss	
$\hbar\omega_p$	Plasma energy $(\sqrt{4\pi N_e r_e^3}\ m_e c^2/\alpha)$	$\sqrt{\rho\,\langle Z/A\rangle} \times 28.816$ eV (ρ in g cm^{-3})
N_e	Electron density	(units of r_e)$^{-3}$
w_j	Weight fraction of the jth element in a compound or mixture	
n_j	$\propto$ number of jth kind of atoms in a compound or mixture	
—	$4\alpha r_e^2 N_A/A$	$(716.408$ g cm$^{-2})^{-1}$ for $A = 1$ g mol^{-1}
X_0	Radiation length	g cm^{-2}
E_c	Critical energy for electrons	MeV
$E_{\mu c}$	Critical energy for muons	GeV
E_s	Scale energy $\sqrt{4\pi/\alpha}\ m_e c^2$	21.2052 MeV
R_M	Molière radius	g cm^{-2}

J. Beringer *et al.*(PDG), PR **D86**, 010001 (2012) (http://pdg.lbl.gov)

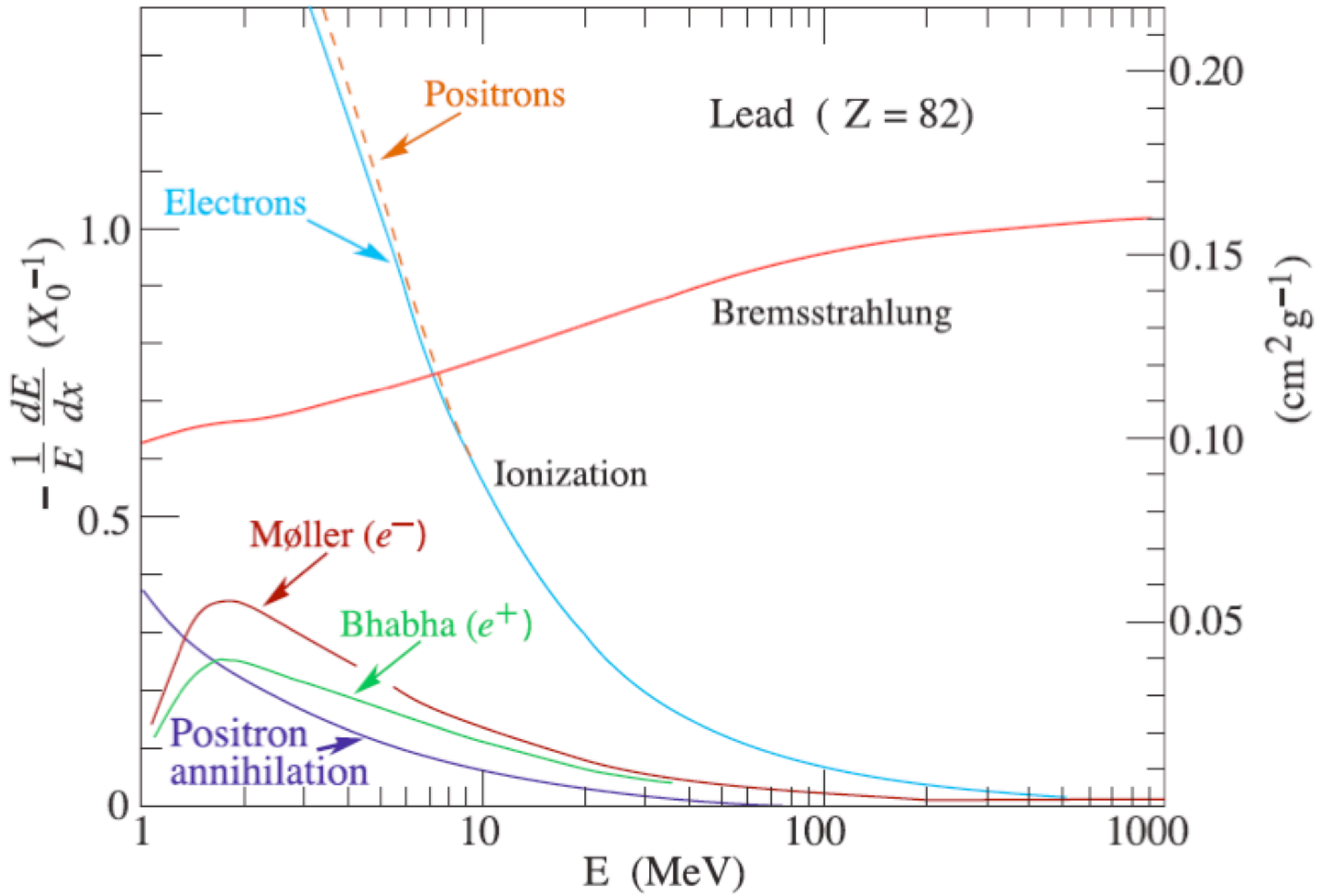

Figure 30.11: Fractional energy loss per radiation length in lead as a function of electron or positron energy. Electron (positron) scattering is considered as ionization when the energy loss per collision is below 0.255 MeV, and as Møller (Bhabha) scattering when it is above. Adapted from Fig. 3.2 from Messel and Crawford, *Electron-Photon Shower Distribution Function Tables for Lead, Copper, and Air Absorbers*, Pergamon Press, 1970. Messel and Crawford use $X_0(\mathrm{Pb}) = 5.82\ \mathrm{g/cm^2}$, but we have modified the figures to reflect the value given in the Table of Atomic and Nuclear Properties of Materials ($X_0(\mathrm{Pb}) = 6.37\ \mathrm{g/cm^2}$).

J. Beringer *et al.*(PDG), PR **D86**, 010001 (2012) (http://pdg.lbl.gov)

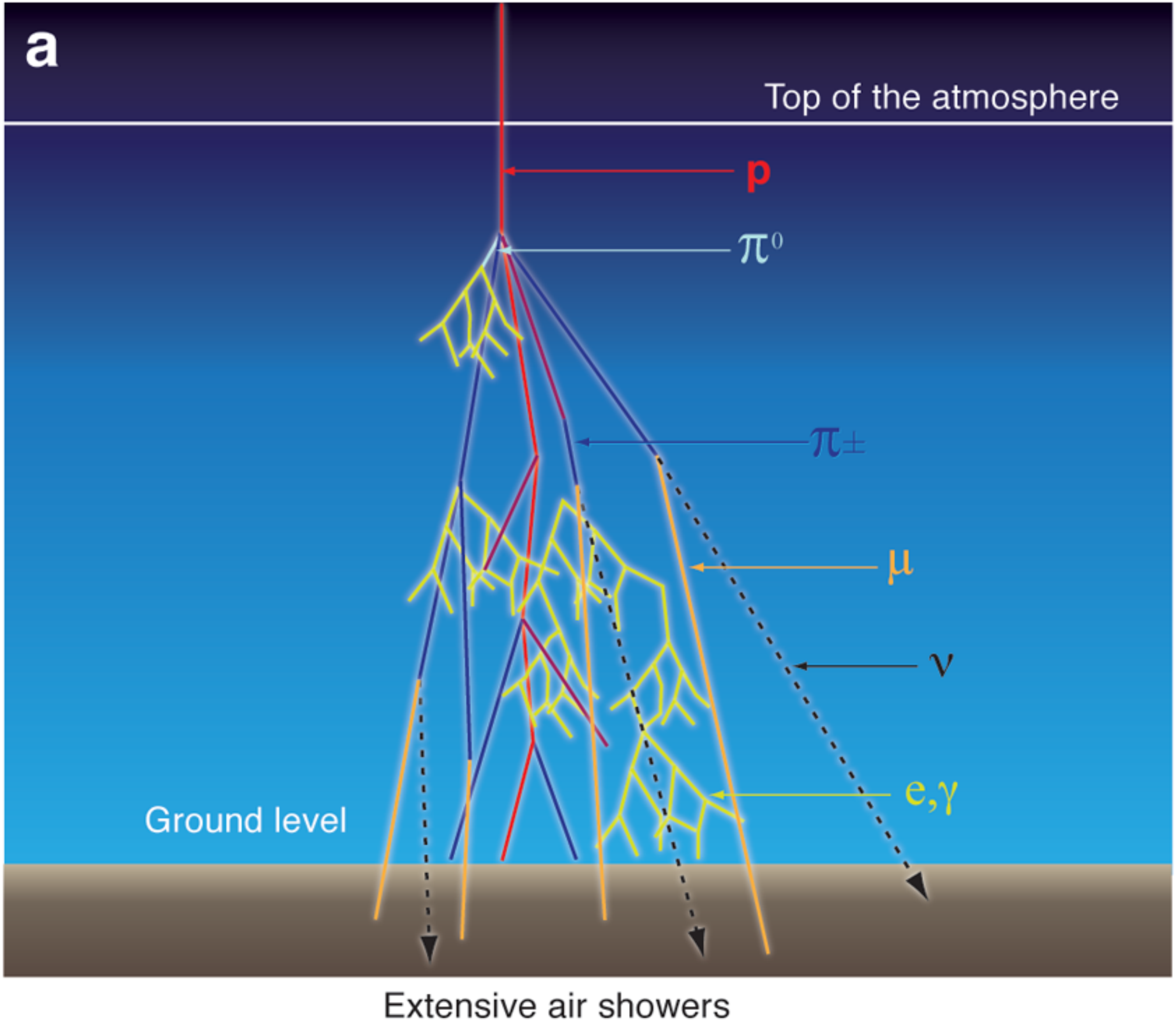
a
Top of the atmosphere
p
π⁰
π±
μ
ν
e,γ
Ground level
Extensive air showers

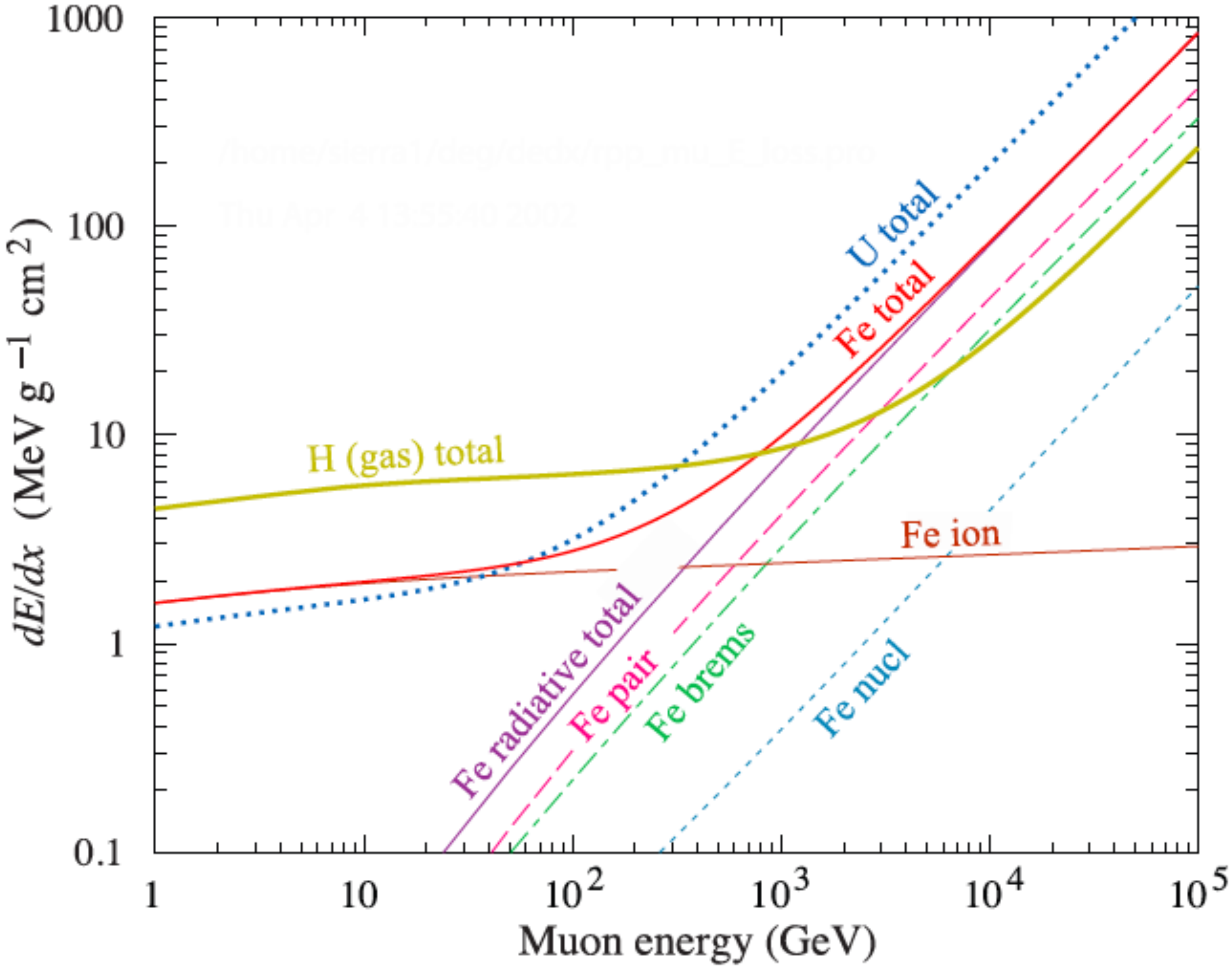

Figure 30.23: The average energy loss of a muon in hydrogen, iron, and uranium as a function of muon energy. Contributions to dE/dx in iron from ionization and the processes shown in Fig. 30.22 are also shown.

J. Beringer *et al.*(PDG), PR **D86**, 010001 (2012) (http://pdg.lbl.gov)

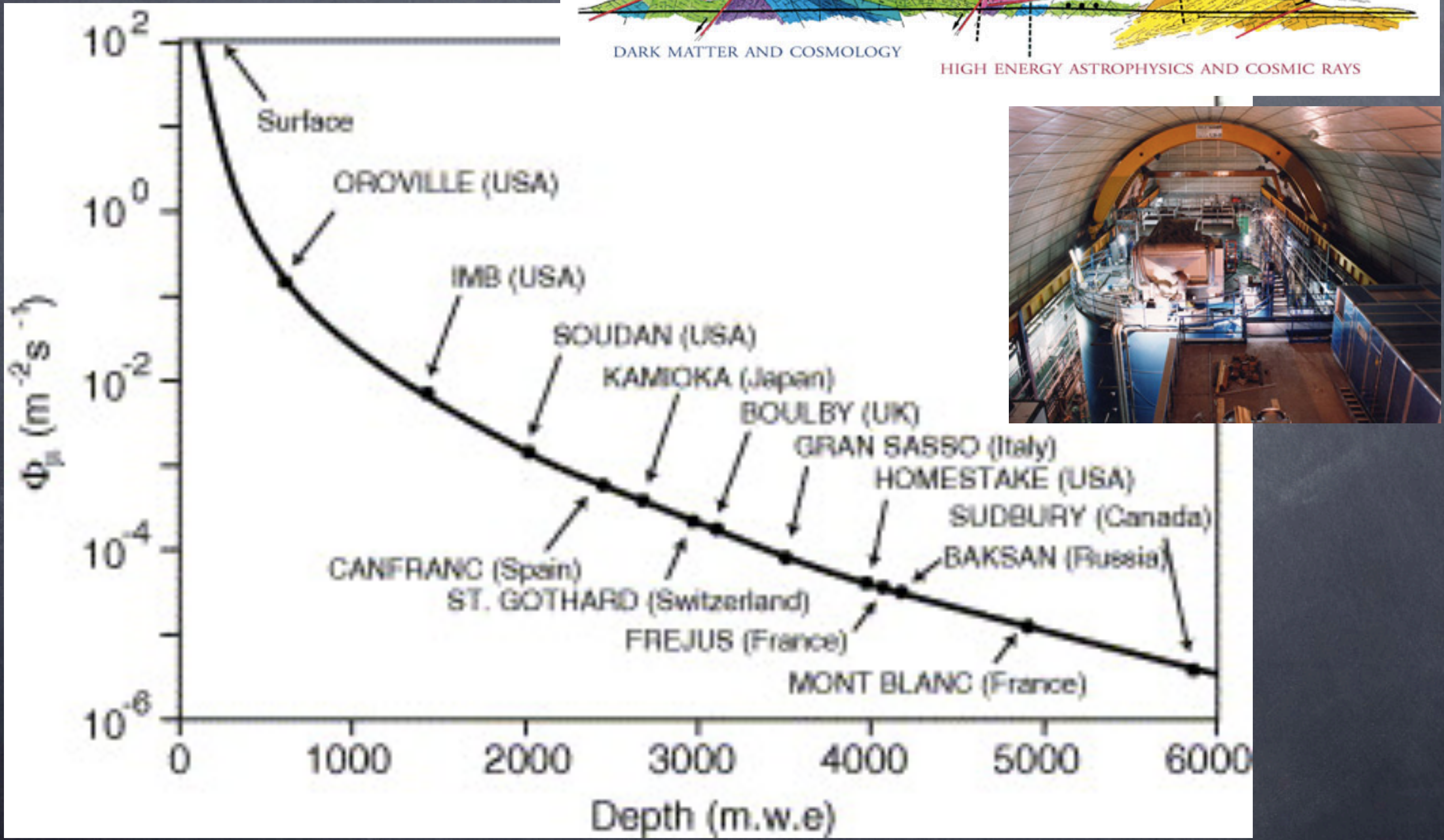

10^2
10^0
10^{-2}
10^{-4}
10^{-6}
Φ_μ ($m^{-2}s^{-1}$)
Surface
OROVILLE (USA)
IMB (USA)
SOUDAN (USA)
KAMIOKA (Japan)
BOULBY (UK)
GRAN SASSO (Italy)
HOMESTAKE (USA)
SUDBURY (Canada)
BAKSAN (Russia)
CANFRANC (Spain)
ST. GOTHARD (Switzerland)
FREJUS (France)
MONT BLANC (France)
0
1000
2000
3000
4000
5000
6000
Depth (m.w.e)

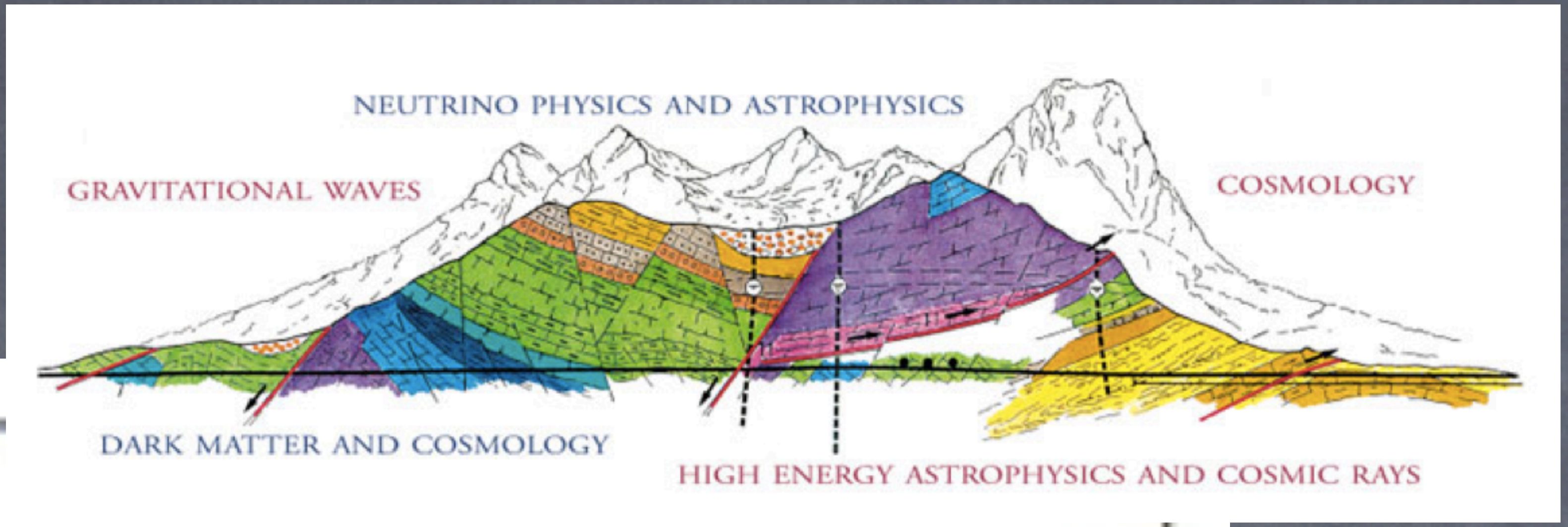

NEUTRINO PHYSICS AND ASTROPHYSICS
GRAVITATIONAL WAVES
COSMOLOGY
DARK MATTER AND COSMOLOGY
HIGH ENERGY ASTROPHYSICS AND COSMIC RAYS